Contents list available at CBIORE journal website

International Journal of Renewable Energy Development

Journal homepage: https://ijred.cbiore.id

Research Article

Future wind speed and energy potential in Togo for the period 2021-2040: Projections from CORDEX-Africa models

Lamboni Batablinlè[1,2,3*], Kassiki Yessou-Gnouyarou[3], Lawson Latévi[3], Kpengou Lorimpo[3], Serge Bazyomo[4], Tchedre Kpéli Esso-ehanam[5], M. Djibibe Moussa Zakari[3], Magolmeena Bannaa[3], Lawin Agnidé Emmanuel[2]

[1]*Department of physics and chemistry, Ecole Normale Supérieure of Atakpamé, Togo*

[2]*Laboratory of Applied Hydrology, National Institute of Water, University of Abomey-Calavi, Benin.*

[3]*Laboratory of Solar Energy, University of Lomé, Togo*

[4]*Laboratoire d'énergies thermique et renouvelables, Université de Ouagadougou, Burkina Faso*

[5]*Laboratory of Thermal and Renewable Energies, Department of Physics, Unit of Training and Research on Exact and Applied Sciences, BP 7021, University Joseph KI- ZERBO, Ouagadougou, Burkina Faso*

Abstract. This study assesses the wind energy potential across Togo by analyzing historical (2001–2020) and future (2021–2040) wind regimes using MERRA-2 reanalysis data and six bias-corrected CORDEX-Africa regional climate models (MIROC, MPI, ICHEC, NOAA, NCC, and IPSL). A Python-based analytical framework was developed to automate data compilation, visualization, and multi-model statistical processing, ensuring reproducibility and computational efficiency. Model performance was evaluated against ground-based observations using a multi-metric validation approach combining R^2, NSE, and RMSE. Results identify MERRA-2 (R^2 = 0.96, NSE = 0.95, RMSE = 0.35) and the RCMs MIROC, MPI, and ICHEC (R^2=0.93–0.95, NSE=0.92–0.94, RMSE<0.45) as the most reliable sources for future wind projections. Seasonal and spatial analyses reveal pronounced heterogeneity across the country. During the rainy season, wind speeds in northern Togo reach 3.8–4.3 m/s, while the southern coastal zone maintains stable year-round winds ranging from 3.9 to 4.5 m/s due to the influence of persistent sea breezes. Future projections for 2021–2040 show an increase in wind speeds of 4–8 %, corresponding to wind power density enhancements of 9–30 %. Peak power density values are projected to reach approximately 52 W/m² in the north, 47 W/m² in the center, and 49 W/m² along the coast. Overall, these findings provide a robust scientific basis for region-specific energy strategies, including the development of hybrid wind–solar systems, targeted coastal installations, and optimized siting of northern wind farms. The results further highlight the potential of wind energy to support national electrification efforts and emerging green hydrogen initiatives, contributing to sustainable development and energy security in Togo.

Keywords: Togo; wind energy potential; seasonal variability; MERRA-2; CORDEX-Africa; regional climate models.

Received: 15th August 2025; Revised: 17th Oct 2025; Accepted: 18th Nov 2025; Available online: 23rd Nov 2025

1. Introduction

Recent advances in wind energy meteorology, coupled with innovations in cost-effective technology, have elevated wind power to a leading position in the global renewable energy sector. While the global potential for wind energy is vast, research efforts have primarily concentrated on well-known wind hotspots such as China (Guo *et al.,* 2019; Abolude *et al.,* 2020), North America (Kulkarni & Huang, 2014; Wang *et al.,* 2016; Breslow & Sailor, 2002), and wind-rich regions in northern Europe and northern Asia (Hueging *et al.,* 2013; Tobin *et al.,* 2015; Bandoc *et al.,* 2018). These regions dominate global installed wind capacity, with China, the United States, and Germany leading the rankings (Abolude *et al.,* 2020). In contrast, most countries in Africa, Oceania, and the Middle East remain at the lower end of the global wind energy spectrum (IRENA, 2020; Chen *et al.,* 2020).

In Africa, existing literature on wind power is relatively robust but still limited, potentially due to the continent's high dependence on hydropower, data scarcity, and ongoing energy crises. Mukasa *et al.* (2013) noted that Africa holds considerable untapped wind energy potential, and early adoption could reduce investment and transition costs. Studies such as Mentis *et al.* (2015) have identified South Africa, Sudan, Algeria, Egypt, Libya, Nigeria, Mauritania, and Tunisia as high-potential countries. Other works have assessed offshore wind energy potential (Olaofe, 2018; Elsner, 2019) or conducted national-scale resource assessments in countries such as Togo (Lamboni et al. 2025, Lamboni *et al.,* 2024), Nigeria (Akinsanola *et al.,* 2017; Udo *et al.,* 2017), Algeria (Boudia *et al.,* 2016), South Africa (Ayodele *et al.,* 2012), Rwanda (Safari & Gasore, 2010), Cameroon (Arreyndip *et al.,* 2016), Chad (Abdraman *et al.,* 2016), Ghana (Asumadu-Sarkodie & Owusu, 2016), Libya (Elmabruk *et al.,* 2014), Burkina Faso (Landry *et al.,* 2017), Morocco (Monjid *et al.,* 2015), Ethiopia (Bekele & Palm, 2009),

* Corresponding author
Email: lambonicharlesbata@gmail.com (L. Batabline)

https://doi.org/10.61435/ijred.2026.61680
ISSN: 2252-4940/© 2026.The Author(s). Published by CBIORE

and Zimbabwe (Hoves *et al.,* 2014). Most of these studies have relied on meteorological station data and/or gridded reanalysis products.

Wind energy potential can be estimated using observational station data, reanalysis datasets, or climate model simulations, with the latter requiring rigorous validation to quantify potential biases. Once validated, model outputs can be applied to assess both current and future wind power potential at local and global scales. Advances in climate modeling now make it possible to analyze the impacts of global warming on wind speed and wind power density (WPD). Global Climate Models (GCMs) and Regional Climate Models (RCMs) have been widely used for this purpose. For example, Zheng *et al.* (2019), using a multi-model ensemble of 12 CMIP5 GCMs, reported an increase in offshore areas with WPD exceeding 400 W/m², but a decrease in regions with WPD above 800 W/m². Similar projections have shown slight declines in U.S. wind speeds by mid-century (Breslow & Sailor, 2002), stability in China's wind speeds through the 21st century (Chen *et al.,* 2012), and mixed patterns across Europe (Tobin *et al.,* 2015; Davy *et al.,* 2018).

In Africa, regional-scale projections have revealed significant variability. Sawadogo *et al.* (2020) projected increases in WPD of up to 20% for 2021–2040 and 2041–2060 using a CORDEX RCM, while Soares *et al.* (2019) reported a north–south contrast with increases in northern Africa and decreases in the south. Fant *et al.* (2016) projected a decline in wind speeds over South Africa by 2050. Over West Africa, however, few studies have employed the most recent generation of climate models (Lamboni *et al.,* 2024). While precipitation and temperature projections are well-documented, wind energy potential remains understudied. Sawadogo *et al.* (2019), using an ensemble of 11 CORDEX RCMs, found that monsoon wind speeds and WPD are likely to increase with warming levels, although such projections remain subject to uncertainties arising from model initialization, parameterization schemes, representation of physical processes, and structural limitations (Tobin *et al.,* 2015; Stouffer *et al.,* 2017; Monrie *et al.,* 2020).

According to Lamboni *et al.* (2025), the analysis of dominant wind directions across Togo reveals substantial spatial and temporal variability, which strongly affects wind energy planning. Site-specific wind characteristics especially stability and seasonal patterns are critical for optimizing turbine placement and ensuring operational efficiency. While locations such as Lomé show relatively stable wind regimes suitable for conventional turbines, sites like Atakpamé, Sotouboua, and Sansanné-Mango exhibit marked seasonal variability, requiring adaptive strategies such as hybrid energy systems or turbines capable of responding to fluctuating wind conditions.

These findings underscore the necessity of extending future studies using climate projection models. The latest phase, CMIP6 (Eyring et al., 2016), offers improved resolution, updated physical parameterizations, and extended scenario pathways. Assessing how well CMIP6 models reproduce wind characteristics over West Africa, and evaluating their projections of future WPD, is essential for informing renewable energy policy and investment strategies. Given Togo's geographic location and growing energy demand, such assessments hold significant value for national planning. Therefore, the objective of this study is to evaluate and project the wind speed and WPD over West Africa with a specific focus on Togo using CMIP6 models. Model performance is first validated against the high-resolution MERRA-2 dataset before assessing future projections.

2. Study area, Methods, data, and Materials

In this section, study area, methods, and data collection, Site Selection, Optimization and Simulation Tools are described.

2.1. Study area

The Republic of Togo, located in West Africa along the Gulf of Guinea, extends from latitudes 6°N to 11°N (Figure 1). It shares its borders with Ghana to the west, Benin to the east, and Burkina Faso to the north. The country's southern coastline stretches for 56 kilometers along the Gulf of Guinea. Encompassing a total area of 54,600 km², Togo exhibits a diverse topography, characterized by undulating hills in the

Fig. 1. Study area

northern regions, a central plateau in the south, and a low-lying coastal plain interspersed with extensive lagoons and marshlands (Batablinlè *et al.* 2025, Lamboni *et al.* 2025). As shown in Figure 1, Togo is divided into five administrative regions arranged from south to north: Maritime, a coastal zone along the Gulf of Guinea that includes the capital Lomé; Plateaux, a mountainous area with the country's highest elevation; Centrale, a transitional zone of hills and valleys; Kara, combining savannas and medium-height mountains; and Savanes, a vast, arid plain forming the northernmost and driest part of the country. Togo faces significant socio-economic challenges, with approximately 69% of rural households currently living below the poverty line. The nation's climate transitions from tropical in the south to savanna in the north. Rainfall patterns in the southern regions follow a bimodal distribution, with the first rainy season extending from mid-March to late July and the second occurring from early September early to mid-November. Conversely, the northern regions experience a single rainy season, typically from May to October (Lamboni *et al,* 2025). During the dry season, spanning from November to March, Togo is influenced by the Harmattan, a dry and dusty trade wind originating from the northeast, which brings cooler temperatures and arid conditions. Additionally, the northern regions are periodically affected by droughts (Lamboni *et al,* 2018, Lawin *et al.* 2019). Togo also benefits from substantial solar radiation throughout the year. Regarding wind energy potential, Togo experiences moderate wind speeds. Higher wind speeds are typically observed in elevated areas, such as coast, the central and northern plateaus (Lamboni *et al.,*2025)

2.2. Data Used

Three sets of data are used in this study. The first set consists of observed data collected from the synoptic stations of Togo. In fact, nineteen meteorological stations have been considered over the historical period 2000-2024. Wind speed observed data were collected at hourly and daily scales. The selection of the time series data was based on the quality of the data collected from various stations. To complement observed values at hourly and daily scales, the second set of data grouping MERRA-2 (Modern Era Reanalysis for Research and Applications Version 2) data available online at https://gmao.gsfc.nasa.gov/reanalysis/MERRA-2/ was used. This data set is very useful in view of the fact that weather stations are limited in number, unevenly distributed, have missing data problem and short period of observation (Asfaw et al. 2018). Missing observed data have been filled using cross validation method following Ioannis, (2017)

Climate Downscaling Experiment (CORDEX) over Africa at 0.44˚ resolution for the period 1950 to 2100 (Giorgi *et al.* 2009) and accessed online (https://www.cordex.org) through user registration. Lamboni *et al.* (2018) employed a set of climate models to construct a multi-model ensemble for their analysis, with the models and their respective acronyms summarized in their study. For a more detailed description of the models, scenarios, and experimental setup, refer to Lamboni *et al.* (2018). The RCP 8.5 is based on the A2r scenario which combines assumptions about high population and relatively slow income growth with modest rates of technological change and energy intensity improvements, leading in the long-term to high energy demand and greenhouse gas emissions in the absence of climate change policies. This set of data is the most up-to-date ensemble of high-resolution Regional Climate Model (RCM) projections. RCM historical data have been used for bias correction. The eight selected models have already been used over Burundi for climate projection (Célestin et al., 2019).

2.3. Methods and materials

The historical climate evaluation was conducted over the period 2000-2024 at hourly scale, seasonal scale and interannual scale. The diurnal analysis of the wind speed and wind direction was done from 7:00 AM to 6:00 PM while the nocturnal analysis was performed from 7:00 PM to 6:00 AM. Furthermore, the spatial distribution of WS and WPD has been adopted using Inverse Distance Weighted (IDW) interpolation method (Célestin *et al.,* 2019, Lamboni *et al.,* 2024).

2.3.1. Bias Correction Method and Change Signal Detection

In this study, Empirical Statistical Downscaling (ESD) and Quantile Delta Mapping (QDM) methods were used for bias correction of RCM data (Lamboni et al., 2024) ESD took wind speed data from 0.44˚ resolution (~50 km × 50 km) to the local scale, while QDM method served to bias adjust and detect changes. This computation was respectively implemented using ESD and Mean Bias Correction (MBC) packages in R program. QDM preserves model-projected change signal in quantiles, while at the same time correcting systematic biases in quantiles of a modelled series based on observed values (Batablinle *et al.* 2018) The conservation of changes follows directly from the quantile perturbation and quantile delta change methods, both of which apply simulated changes in quantiles overtop observed historical series (Lamboni *et al.*2024).

2.3.2. Wind speed variation with height

Wind speed near the ground changes with height. This requires an equation that predicts the wind speed at one height according to a measured speed at another. The most common expression for the variation of wind speed with the height is the power law having the following form (Mahyoub et al., 2006):

$$\frac{v_2}{v_1} = \left(\frac{z_2}{z_1}\right)^{\alpha} \quad (1)$$

Where v_2 and v_1 stand for the mean wind speeds at heights z_2 and z_1, respectively. The exponent α depends on factors such as surface roughness and atmospheric stability. Numerically, it lies in the range of 0.05–0.5, with the most frequently adopted value being 0.14 which is widely applicable to low surfaces and well-exposed sites (Lamboni *et al.,* 2025).

The hub heights of 50 m, 90 m, and 150 m were selected for this assessment to align with current and future technological standards in the wind energy industry. The 50 m height represents the characteristic hub height of older or smaller turbine models and allows for comparison with historical studies (Akinsanola *et al.,* 2017). The 90 m height is representative of modern commercial wind turbines, which are now standard for most utility-scale projects (Allouhi *et al.,* 2017). Finally, the 150 m height is increasingly considered for

Table 1
Performance metrics of MERRA-2 and bias-corrected CORDEX-Africa RCMs against ground observations (Period: 1981-2020).

Model/Dataset	R^2	NSE	RMSE
MERRA-2	0.96	0.95	0.35
MIROC	0.94	0.93	0.41
MPI	0.93	0.92	0.43
ICHEC	0.95	0.94	0.39
NOAA	0.87	0.85	0.58
NCC	0.76	0.72	0.81
IPSL	0.74	0.70	0.85

next-generation turbines and provides critical insight into the future scalability and potential of wind energy in Togo, as taller turbines can access stronger, more consistent wind resources (IRENA, 2023).

2.3.3. Wind Power density function and average error value

It is well known that the power of the wind at speed through a blade sweep area (A) increases as the cube of its velocity and is given by (Lamboni *et al*., 2024).

$$P(v) = \frac{1}{2} A \rho v^3 \quad (2)$$

Where P(v) is the power of the wind (in W), ρ stands for the air density (in kg·m−3), A is representing the swept area (in m2) and v , the wind speed (in m·s−1).

Therefore, the wind power density $P_D(v)$ (in $W \cdot m^{-2}$) is given by the following equation

$$P_D(v) = \frac{1}{2} \rho v^3 \quad (3)$$

The correlation coefficient (R) was used to analyze the accuracy and deviation between the simulated and observed data which was quantified as follow:

$$R = \frac{\frac{1}{N}\sum_{i=1}^{N}(f_n - \overline{f})(r_n - \overline{r})}{\sigma_f \sigma_r} \quad (4)$$

The Nash–Sutcliffe Efficiency (NSE), and the Root Mean Square Error (RMSE) were also used to evaluate the performance of the model. These statistical indicators quantify the accuracy and deviation between the simulated and observed data (Batablinle *et al.,* 2018).

To analyze these parameters, wind direction data were processed and visualized using Python, employing packages such as pandas for data handling, numpy for numerical computations, matplotlib and seaborn for static plotting, plotly for interactive visualization, and pytest for testing. All calculations were performed using Python scripts to ensure reproducibility and computational efficiency. In this framework, the Wind Power Density (WPD) function and average error values were computed to assess wind energy potential.

3. Results

3.1. MERRA-2 and RCM Performance

To ensure the reliability of wind speed projections across Togo, the performance of the reanalysis dataset MERRA-2 and six bias-corrected CORDEX-Africa regional climate models (MIROC, MPI, ICHEC, NOAA, NCC, and IPSL) was systematically evaluated against ground-based observations using a multi-metric framework. The assessment incorporated the Coefficient of Determination (R^2), Nash–Sutcliffe Efficiency (NSE), and Root Mean Square Error (RMSE), providing a comprehensive measure of each model's skill (Table 1).

MERRA-2 exhibited excellent agreement with observations, achieving R^2=0.96, NSE = 0.95, and RMSE=0.35, confirming its reliability as a reference dataset for subsequent analyses. Among the RCMs, MIROC, MPI, and ICHEC consistently demonstrated high performance, with R^2 values between 0.93 and 0.95, NSE between 0.92 and 0.94, and RMSE below 0.45 m/s, accurately reproducing historical wind patterns across all climatic regions of Togo. In comparison, the NOAA model showed moderate skill (R^2 = 0.87, NSE =0.85), while NCC and IPSL underperformed, with lower R^2 (0.74–0.76), lower NSE (0.70–0.72), and higher RMSE (0.81–0.85), reflecting a systematic underestimation of wind speeds.

Based on this evaluation, MIROC, MPI, and ICHEC were identified as the most reliable models and prioritized for future wind projections and multi-model mean calculations, whereas the lower-performing models (NCC and IPSL) were retained for transparency but interpreted with caution in subsequent analyses.

3.2. Comparative Analysis of Wind Speed Projections in Togo (2021-2040) by Climate Models

The assessment of wind energy potential across Togo, using multiple CORDEX-Africa climate model outputs, consistently reveals a pronounced north–south gradient in average wind speeds. At 50 m above ground level (Figure 2), wind resources are already significant in the northern region, where speeds range between 2.8 and 5.3 m/s. This indicates an exceptional potential for wind energy development. Among the models, ICHEC provides the most optimistic projections (up to 5 m/s), whereas NOAA remains more conservative (2–6.1 m/s). Such sustained high wind speeds suggest that large-scale wind farms could operate efficiently in this area without requiring specialized low-speed technologies.

In the central region, wind speeds range from 2.5 to 5 m/s, with MIROC reaching 4.3 m/s and NOAA presenting the lowest credible values (2.6–4.7 m/s). Although lower than in

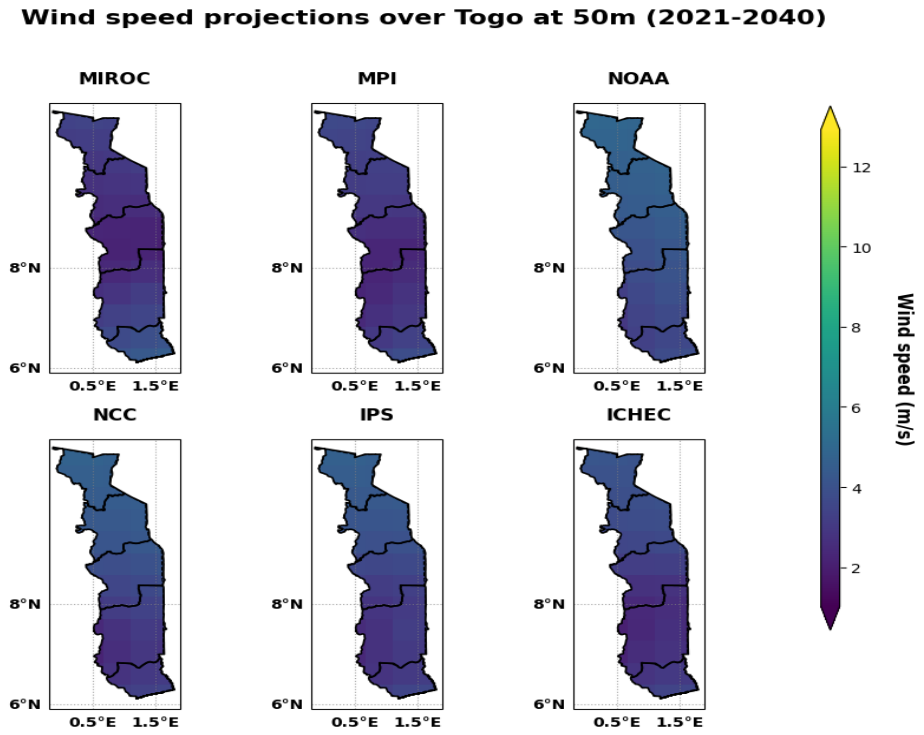

Fig 2. Spatial distribution of Wind Speed Projections at 50m in Togo According to Six Climate Models (2021-20240).

the north, these values remain suitable for energy production if turbines optimized for moderate wind regimes are selected. In contrast, the southern region including the coastal belt shows more potential, with average wind speeds between 3 and 5.6 m/s. In this case, the use of low cut-in speed turbines or solar–wind hybrid systems would be required to achieve economic viability. It is worth noting that several independent studies highlight that, despite these modest mean speeds, the coastal fringe benefits from persistent maritime breezes during the rainy season (Lamboni *et al.*, 2024, Lamboni *et al.*, 2025).

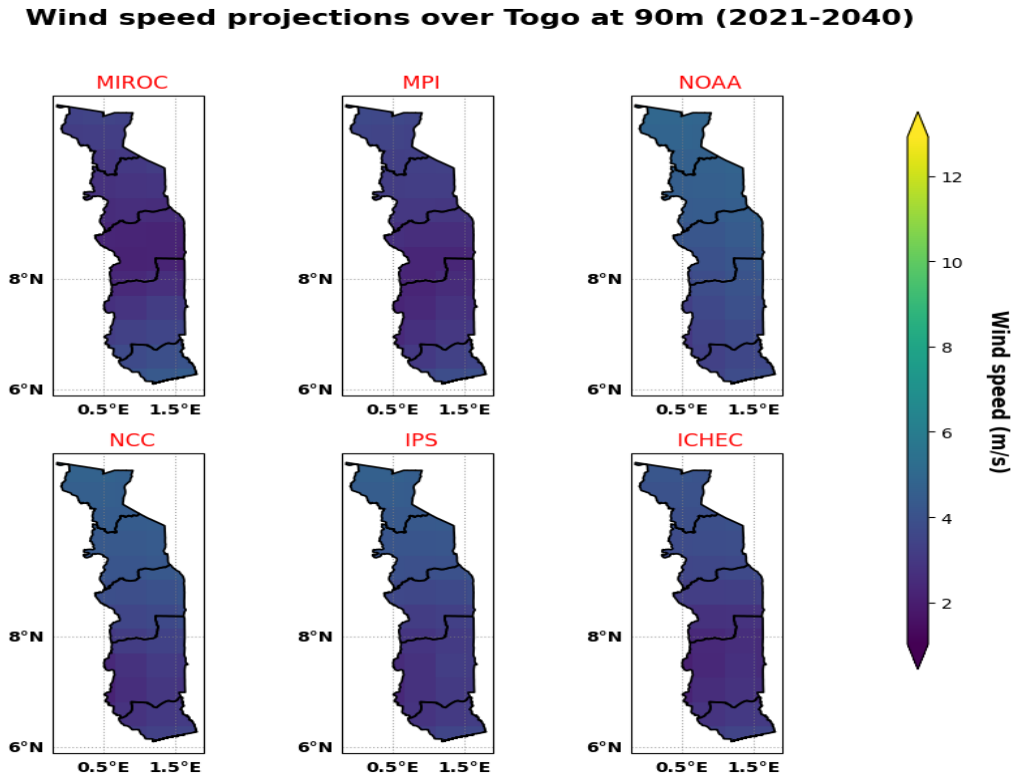

Fig 3. Spatial distribution of Wind Speed Projections at 90m in Togo According to Six Climate Models (2021-20240)

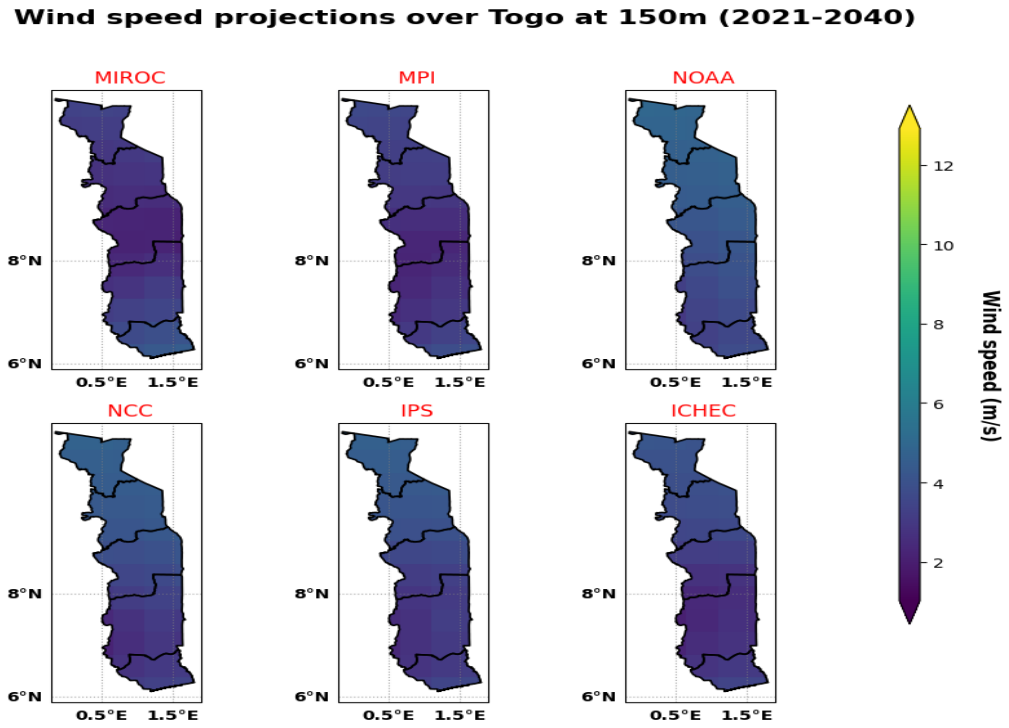

Fig 4. Spatial distribution of Wind Speed Projections at 150m in Togo According to Six Climate Models (2021-20240).

These local winds may enhance energy production beyond the regional averages represented in the climate models.

Raising the hub height to 90 m (Figure 3) reveals both increased potential and greater divergence between models. In the northern region, the most reliable datasets (MIROC, MPI, and ICHEC) as identified in Table 1 consistently indicate wind speeds between 3.2 and 5.3 m/s, confirming the excellent suitability of this area for the development of high-capacity wind farms. Conversely, NCC and IPS produce unrealistically low estimates (< 4 m/s), likely due to systematic underestimation or data artifacts, and should be excluded unless validated by independent measurements. In the central region, a broader credible range is observed (4–8 m/s). MIROC and ICHEC project the upper end (6–8 m/s), while MPI and NOAA suggest more conservative values (4–6 m/s). This variability underscores the importance of local wind measurement campaigns prior to major investments. In the south, the reliable models indicate speeds between 2 and 4.5 m/s. NCC and IPS continue to report implausible near-zero values.

At 150 m (Figure 4), the spatial pattern remains broadly consistent, but higher hub heights further reinforce the competitiveness of northern sites. MIROC, MPI, and ICHEC maintain their consensus with speeds of 2–6.3 m/s, while NOAA projects slightly lower values (2.5–5.2 m/s) but still indicates high feasibility for energy development. NCC and IPS continue to underestimate wind potential (2.1–4.6 m/s and 2–4 m/s, respectively), reinforcing the need for careful model selection. In the central zone, realistic projections span 2–6.3 m/s, with MIROC and ICHEC at the higher end and MPI and NOAA providing more moderate outputs. In the south, consistent models again record 4–6.5 m/s, supporting targeted deployment of solar–wind hybridization strategies. Within this southern context, two sub-regions are particularly noteworthy: the coastal fringe, where seasonal sea breezes enhance energy production, and the orographically influenced Plateau highlands, where localized acceleration may create niche wind opportunities (Lamboni *et al.,* 2025). Both areas could support site-specific projects if combined with appropriate technology choices and localized validation.

Considering the findings from the previous section, which revealed divergences among models depending on both height and the specific model considered despite a generally good overall agreement the subsequent analysis is based on the multi-model average of six CORDEX-Africa models at a 50 m hub height. This approach helps to mitigate individual model biases, smooth out extreme values, and provide a robust and representative estimate of regional wind conditions. The analysis in the following section relies on these multi-model averages at 50 m to examine in detail the spatial and seasonal characteristics of wind resources. This choice ensures coherent comparisons across regions and seasons and supports reliable planning for small- to medium-scale wind energy projects. This strategy aims to identify robust regional patterns by reducing the influence of individual model uncertainties and provides a solid basis for a more accurate assessment of national wind energy potential.

3.3. Monthly Wind Speed Analysis and Seasonal Wind Speed Analysis Across Togo using Mean-Models

To understand the wind dynamics across Togo, the analysis was conducted at two complementary scales in this section. The first sub-section, Monthly Wind Speed Analysis, focuses on the variation of wind speeds on a month-to-month basis, highlighting regional differences and temporal trends throughout the year. The second sub-section, Seasonal Wind Speed Analysis Across Togo using Mean-Models, synthesizes these monthly variations into broader seasonal patterns, providing insights into the overall wind climate during the dry

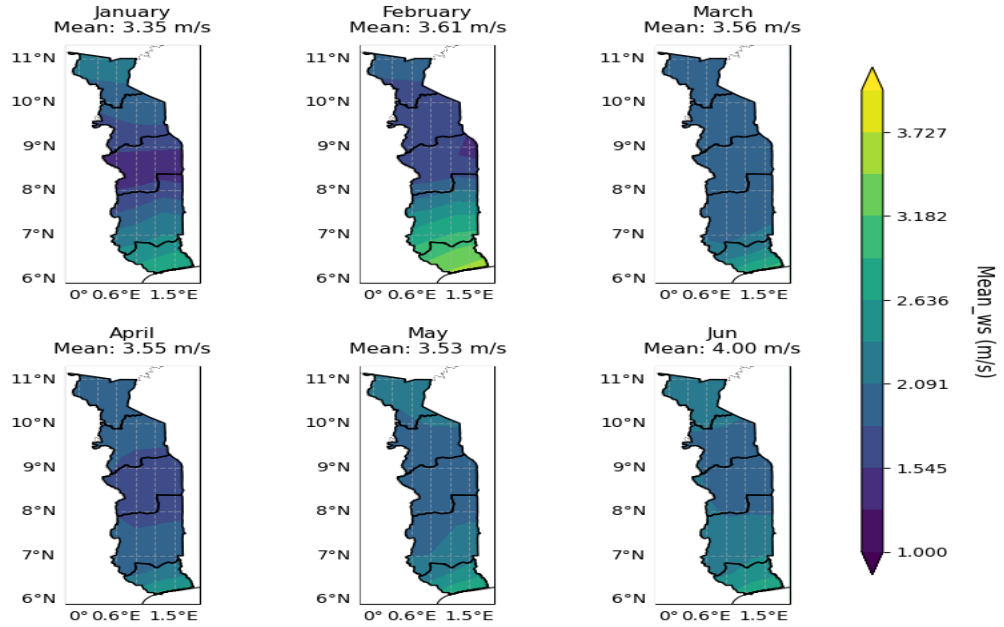

Fig 5. Spatial distribution of monthly mean wind speed during the future period, according to Mean-Models (2021–2040) at 50 m.

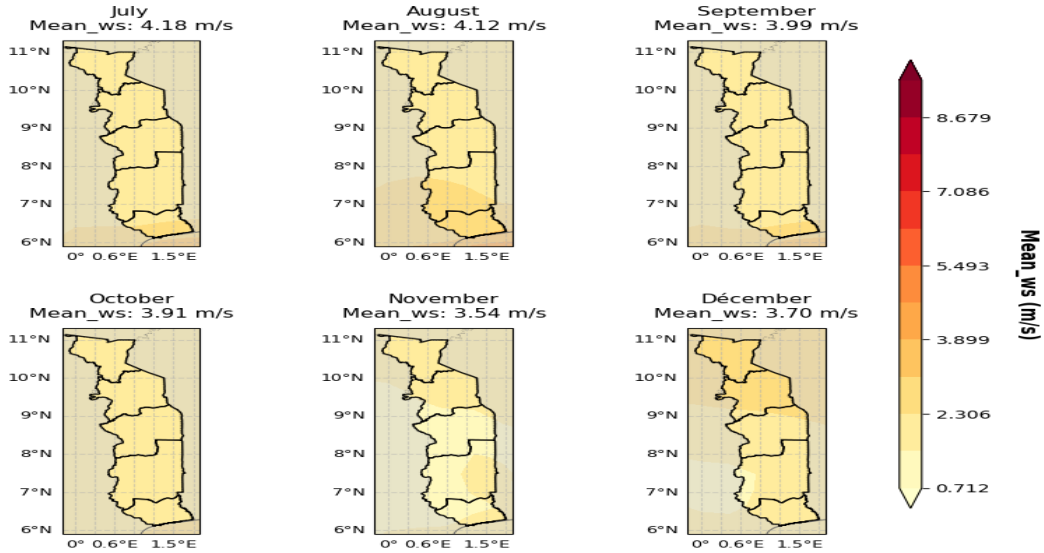

Fig 6. Spatial distribution of annual mean wind speed during the future period, according to Mean-Models (2021–2040) at 50 m.

and rainy periods. Together, these analyses offer a comprehensive view of wind behavior in Togo, from fine-scale monthly fluctuations to aggregated seasonal trends, facilitating a better understanding for applications such as renewable energy planning and climate assessment.

3.3.1. Monthly Wind Speed Analysis Across Togo using Mean-Models

The spatial and temporal distribution of mean wind speeds across Togo reveals pronounced seasonal variations, with marked differences between the northern, central, and southern zones. Between January and March (Figure 5), wind speeds remain at their weakest annual levels. January shows an average of 3.35 m/s, the lowest in the dataset, significantly limiting the viability of stand-alone wind projects. February's mean of 3.61 m/s and March's 3.56 m/s indicate minimal change, with any exploitation requiring highly specialized low-wind turbines or hybridization with solar energy. From April to June (Figure 6), there is a gradual increase in wind potential. April's 3.55 m/s remains modest, but may holds steady at 3.53 m/s, showing little seasonal boost. However, by June, the average climbs sharply to 4.00 m/s, signaling the onset of a more favorable period for wind exploitation especially in elevated areas of the Plateaux in south region and in the northern savanna regions.

From July to September (Figure 6), wind speeds are relatively higher compared to most other months. July shows a national mean of 4.18 m/s, with the northern region maintaining slightly stronger winds than the center, suggesting moderate viability for low-cut-in-speed turbines. In August, the average speed slightly declines to 4.12 m/s, but the spatial pattern remains consistent, sustaining moderate energy potential in the north and southern. By September, the mean

speed decreases further to 3.99 m/s, reflecting the gradual transition toward the calmer months of the year; nonetheless, localized highland areas, particularly in the south. From October to December (Figure 6), there is a progressive weakening of the wind resource. October records 3.91 m/s, maintaining marginal viability for specialized wind systems in the northern highlands. In November, speeds drop to 3.54 m/s, marking one of the least favorable months for wind generation nationwide, with the north and southern retaining a slight advantage. December sees a modest recovery to 3.70 m/s, which, although still low for large-scale deployment, can sustain hybrid solar–wind systems, particularly in the coastal zone where several independent studies confirm seasonal sea-breeze reinforcement.

In summary, the northern and south regions consistently outperform the rest of the country, maintaining higher wind speeds throughout the year and offering the best potential for wind energy, particularly from June to September. The central zone shows moderate seasonal variability, with potential peaking in mid-year. The southern coastal belt, despite generally more stable average speeds, benefits from localized wind systems such as sea breezes, which, as confirmed by numerous studies, can increase production potential during certain months. Therefore, an optimized wind strategy in Togo should combine large-scale northern projects with targeted exploitation of coastal and mountain microclimates, complemented by solar hybridization during low-wind months.

3.3.2. Seasonal Wind Speed Analysis Across Togo using Mean-Models

Tables 2, 3, and 4 present the seasonal variability of wind speed across Togo for the projection period 2021–2040. The results highlight a clear contrast between the dry and rainy seasons, both in terms of intensity and spatial distribution. During the dry season, wind speeds are relatively lower and more stable, ranging from 2.8 to 3.8 m/s across the country. The southern region consistently records the highest wind speeds (3.5–3.8 m/s), mainly due to its coastal location, which favors the development of sea breezes and other coastal wind systems. The central region experiences moderate wind speeds (3.3–3.7 m/s), whereas the northern region registers the lowest values (2.8–3.5 m/s). Overall, wind activity during this period is concentrated in the southern coastal zone, suggesting that this area may offer more stable wind energy potential during the dry months.

In contrast, the rainy season is characterized by a marked intensification of wind speeds across all regions, particularly between June and August. The northern and central regions experience the highest wind speeds, often exceeding 4.0 m/s, with peaks of 4.3–4.4 m/s observed in July. The southern region remains relatively stable around 4.0 m/s. This northward increase in wind intensity during the rainy season is likely associated with seasonal atmospheric circulation, especially the West African Monsoon, which brings stronger, moisture-laden winds inland (Lamboni et al., 2024). Consequently, the wind regime shifts from a coastal dominance during the dry season to a northern dominance during the wet season, reflecting the dynamic and spatially heterogeneous nature of wind patterns over Togo.

These spatial and seasonal variations in wind speed have significant implications for both wind energy development and climate studies. The southern region provides steady but moderate wind potential throughout the year, making it suitable for continuous small- to medium-scale energy generation. In contrast, the northern and central regions exhibit pronounced seasonal peaks that could be strategically harnessed for seasonal power production or integrated into hybrid renewable energy systems. These findings are consistent with Lamboni et al. (2025) in their study *Modeling and Optimization of Hybrid Hydro–Solar–Wind Systems for Green Hydrogen Production in Togo,* which highlights south region as a promising site for hybrid wind–solar systems. To fully leverage Togo's renewable energy potential, the study underscores the importance of energy storage solutions,

Table 2
Estimated Wind Speed Distribution by Region during the Dry Season (November–April) at 50m

Month	North (m/s)	Center (m/s)	South (m/s)	National Mean (m/s)
November	3.0 – 3.5	3.3 – 3.6	3.5 – 3.8	3.54
December	3.0 – 3.4	3.4 – 3.6	3.5 – 3.8	3.70
January	2.8 – 3.3	3.2 – 3.5	3.5 – 3.7	3.35
February	3.1 – 3.5	3.4 – 3.7	3.6 – 3.8	3.61
March	3.0 – 3.4	3.3 – 3.6	3.5 – 3.7	3.56
April	3.1 – 3.4	3.3 – 3.6	3.5 – 3.7	3.55

Table 3
Estimated Wind Speed Distribution by Region during the Rainy Season (May–October) at 50 m

Month	North (m/s)	Center (m/s)	South (m/s)	National Mean (m/s)
May	3.1 – 3.5	3.3 – 3.6	3.5 – 3.8	3.53
June	3.8 – 4.3	3.9 – 4.1	4.0 – 4.3	4.00
July	4.1 – 4.4	4.2 – 4.3	4.2 – 4.4	4.18
August	4.0 – 4.3	4.0 – 4.2	4.1 – 4.3	4.12
September	3.8 – 4.2	3.9 – 4.1	4.0 – 4.2	3.99
October	3.6 – 3.9	3.8 – 4.0	3.9 – 4.1	3.91

Table 4
Seasonal Summary of Wind Speed Characteristics by Region

Region	Dry Season (Nov–Apr)	Rainy Season (May–Oct)	Peak Wind Period
North	2.8 – 3.5 m/s	3.8 – 4.4 m/s	June – August
Center	3.3 – 3.7 m/s	3.8 – 4.3 m/s	June – August
South	3.5 – 3.8 m/s	3.9 – 4.3 m/s	Year-round (peak in rainy season)

Table 5
Estimated Wind Power Density during Dry Season (November–April) at 50 m

Month	North (W/m²)	Center (W/m²)	South (W/m²)	National Mean (W/m²)
November	16.5 – 26.2	21.5 – 28.5	26.2 – 32.9	27.8
December	16.5 – 24.6	24.6 – 28.5	26.2 – 32.9	31.7
January	13.5 – 22.0	19.6 – 26.2	26.2 – 30.4	23.5
February	18.2 – 26.2	24.6 – 31.7	28.5 – 32.9	29.4
March	16.5 – 24.6	22.0 – 28.5	26.2 – 30.4	28.2
April	18.2 – 24.6	22.0 – 28.5	26.2 – 30.4	27.9

Table 6
Estimated Wind Power Density during Rainy Season (May–October)

Month	North (W/m²)	Center (W/m²)	South (W/m²)	National Mean (W/m²)
May	18.2 – 26.2	22.0 – 28.5	26.2 – 32.9	27.6
June	32.9 – 48.8	35.4 – 41.3	39.2 – 48.8	39.2
July	45.3 – 52.2	44.4 – 47.7	44.4 – 52.2	44.7
August	39.2 – 58.8	39.2 – 44.4	41.3 – 48.8	58.0
September	32.9 – 44.4	35.4 – 41.3	39.2 – 44.4	38.0
October	28.5 – 35.4	32.9 – 39.2	35.4 – 41.3	35.9

Table 7
Seasonal Wind Power Density Summary by Region

Region	Dry Season (W/m²)	Rainy Season (W/m²)	Peak Energy Period
North	13.5 – 26.2	32.9 – 52.2	June – August
Center	19.6 – 31.7	32.9 – 47.7	June – August
South	26.2 – 32.9	35.4 – 48.8	Year-round

hybrid integration, and targeted policy support to optimize the green hydrogen production and supply chain. These strategies are essential to ensuring a sustainable and reliable energy future for Togo, capable of meeting both current and future energy demands.

This spatial and temporal distribution underscores the importance of region-specific strategies for optimizing wind energy planning and resource management in Togo.

3.4. Seasonal Wind power density Analysis Across Togo using Mean-Models

Building on the previous section, which examined the seasonal variability of wind speed across Togo, this section focuses on the corresponding wind power density estimates. Tables 5, 6, and 7 present the estimated wind power densities for both the dry and rainy seasons during the projection period 2021–2040, highlighting clear seasonal contrasts that mirror the wind speed patterns described earlier.

During the dry season (November–April), wind power densities remain generally low to marginal, ranging between 16 and 33 W/m² nationwide. The southern region exhibits the highest values, between 26.2 and 32.9 W/m², reflecting its slightly stronger and more stable coastal winds. The central region shows moderate values (19.6–31.7 W/m²), while the northern region records the lowest power densities (13.5–26.2 W/m²). These values correspond well with the lower wind speeds observed during this period, indicating limited but consistent wind energy potential along the coast, and weaker inland resources.

In contrast, the rainy season (May–October) reveals a marked increase in wind power density across all regions (Table 6). National averages rise to the 28–58 W/m² range, with the highest values occurring between June and August, particularly in the northern and central regions where wind speeds frequently exceed 4 m/s. The northern region reaches power densities of up to 52.2 W/m² in July, while the southern region maintains relatively stable values between 35.4 and 48.8 W/m² throughout the season. This seasonal peak corresponds to the strengthening of the West African Monsoon circulation, which brings more intense inland winds (Lamboni *et al*, 2025).

The seasonal summary (Table 7) clearly shows that wind energy potential follows a northward gradient during the rainy season, contrasting with the southern coastal dominance observed in the dry season. The southern region benefits from year-round to fair energy resources, making it suitable for continuous, small- to medium-scale wind energy exploitation. Meanwhile, the northern and central regions experience pronounced seasonal peaks, offering opportunities for strategic or hybrid energy planning, such as combining wind with solar or hydropower during peak months.

Overall, the analysis of wind power density reinforces the patterns identified in the wind speed assessment, demonstrating the spatially heterogeneous and seasonally dynamic nature of Togo's wind energy potential. This underlines the importance of region-specific energy development strategies, leveraging coastal stability in the south and seasonal peaks in the north and center to optimize wind resource utilization.

3.5. Projected Seasonal Changes in Wind Speed and Energy Density over Togo (2021–2040)

Building upon the previous section on seasonal wind speed variability, it is also essential to examine how projected changes in wind regimes may translate into energy potential. Figure 7 presents the seasonal median wind speeds for the baseline period (2001-2020) and the future period (2021–2040) across the three major climatic regions of Togo. A consistent increase in wind speed is observed across all regions and seasons, with the most pronounced changes occurring in the northern region, where median wind speeds are projected to rise by approximately 8 % during both the dry and rainy seasons. The central region follows with a 6 % increase, while

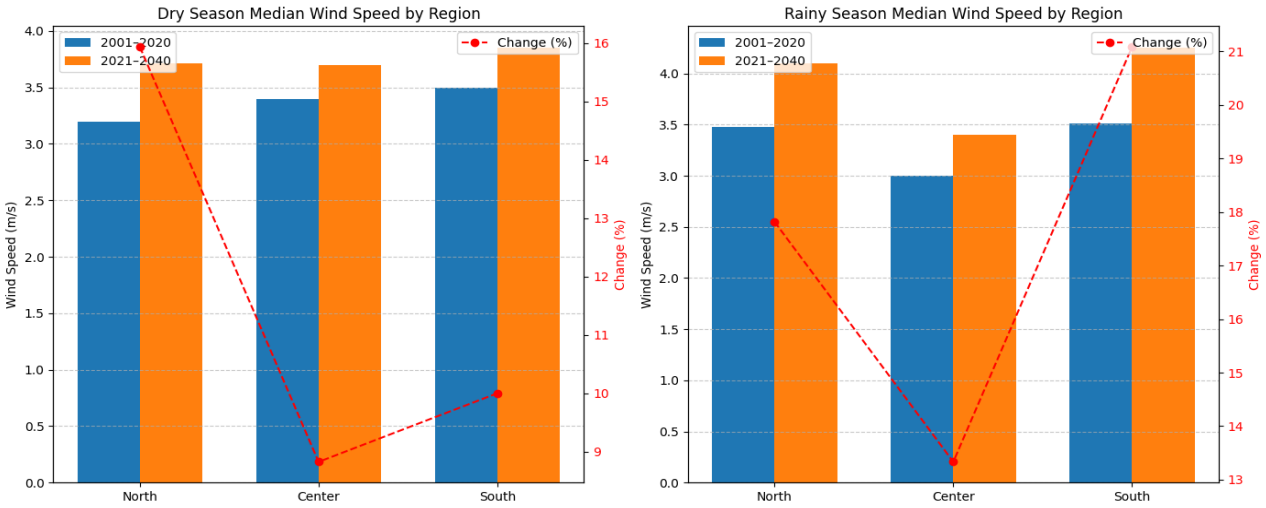

Fig 7. Seasonal Median Wind Speed (m/s) by Region for the Reference (2001–2020) and Future (2021–2040) Periods.

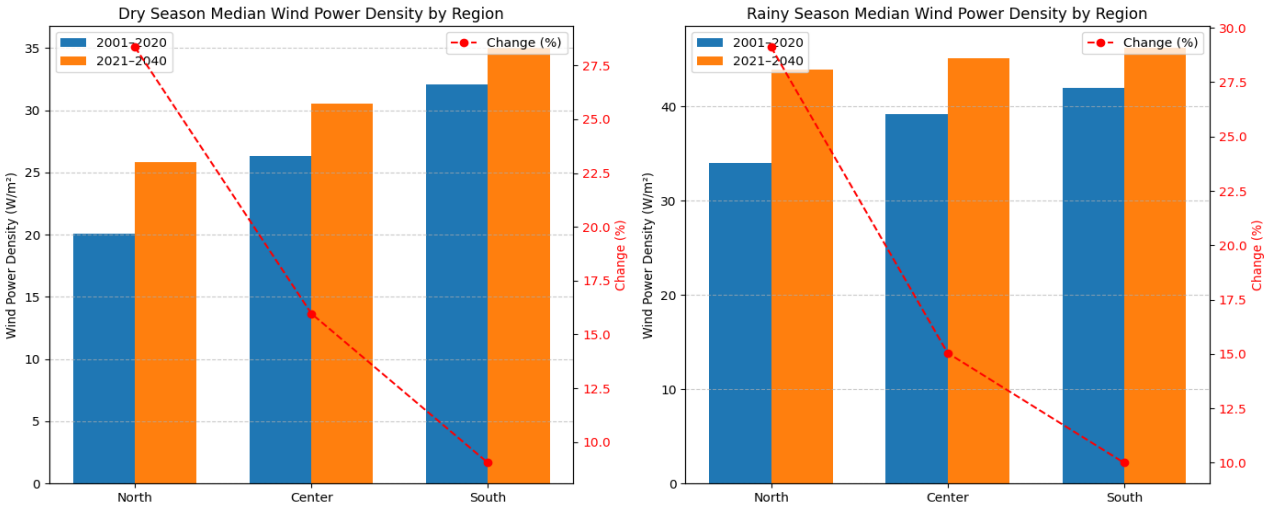

Fig 8. Seasonal Median Wind Power Density (W/m²) by Region for the Reference (2001–2020) and Future (2021–2040) Periods

the southern coastal zone shows a more moderate but still significant increase of around 4 %.

These changes in wind speed lead to a substantial amplification of wind power density (WPD), as shown in Figure 8. Because WPD scales with the cube of wind speed, even modest increases in velocity translate into disproportionate energy gains. In the northern region, WPD is projected to increase by nearly 30 % during both seasons, reflecting its strong sensitivity to intensified monsoonal flows. The central region records a 15–16 % increase, while the southern region shows a 9–10 % rise, maintaining its role as a stable year-round wind resource zone.

Overall, these results indicate a shift toward enhanced wind energy potential across Togo by 2040, particularly in the northern and central regions during the rainy season. This evolution underscores the importance of integrating future wind projections into national energy planning and infrastructure development, especially for hybrid renewable systems that can capitalize on seasonal peaks.

4. Discussion

This study combines a robust model evaluation with a seasonal spatial analysis to assess Togo's wind energy potential, bridging observational validation with future climate projections. The high agreement between MERRA-2 reanalysis and ground observations (R^2 = 0.96), along with the strong performance of bias-corrected CORDEX-Africa RCMs particularly MIROC, MPI, and ICHEC confirms the reliability of these datasets for national-scale wind assessments.

Based on the multi-model ensemble mean, a persistent north–south gradient in wind speeds is observed: northern sites reach 3–5.3 m/s at heights ≥90 m, central sites record 2.5–4.8 m/s, and southern sites reach 3–5.6 m/s, locally enhanced by coastal sea breezes and orographic effects in the Plateaux highlands (south of Togo). Seasonal analysis highlights peak wind speeds from June to September, with the national July mean at 4.18 m/s. By December, wind speeds decline by 23 % in the north, show a more gradual decrease in

the central region, and decrease by 14 % and 11 % in the southern and coastal zones, respectively. This pattern emphasizes the greater stability of maritime-influenced areas.

Wind Power Density (WPD) patterns reinforce these trends, increasing from 52.3 W/m² in January to a peak of 59.4 W/m² in August, with maximum values exceeding 58 W/m² in optimal northern and coastal locations. These spatial and seasonal variations underline the need for region-specific wind energy strategies and the integration of hybrid systems in areas with moderate wind regimes. The southern region, with its stable year-round moderate winds, is well suited for continuous small- to medium-scale power generation, while the northern and central regions, characterized by strong seasonal peaks, offer opportunities for seasonal power production and hybrid renewable systems.

These findings are consistent with Lamboni et al. (2025), Lamboni et al. (2024), whose study *Modeling and Optimization of Hybrid Hydro–Solar–Wind Systems for Green Hydrogen Production in Togo* identified the southern region as a promising site for hybrid wind–solar systems. The authors emphasize the critical role of energy storage solutions, hybrid integration, and targeted policy support to optimize the green hydrogen production and supply chain, ensuring a sustainable and reliable energy future for Togo.

The present results also align with broader regional trends. In Africa, Sawadogo et al. (2020) projected up to 20 % increases in WPD at 50 m over South Africa by 2050, while Akintomide et al. (2021) reported decreases in the Sahel but gains in the Guinea coast and Savannah subregions, with high inter-model agreement. These patterns indicate that coastal and maritime-influenced areas, such as southern Togo, are among the most favorable for commercial wind development. Similarly, multi-model CMIP5 ensemble analyses have shown increases in offshore WPD > 400 W/m² globally, particularly in lower latitudes, although reductions were noted in areas already exceeding 800 W/m² (Breslow & Sailor, 2002; Chen et al., 2012), while Lamboni et al. (2024, 2025) projected future increases in monthly wind speed and WPD across the Mono Basin under both RCP4.5 and RCP8.5 scenarios, with the south experiencing the highest gains (9–10 %) and the central region showing increases of 15–16 %, consistent with the patterns observed in this study. This convergence indicates that southern and coastal Togo fits within a broader regional pattern of maritime wind stability and enhancement.

Globally, regional contrasts emerge. For example, Breslow and Sailor (2002) projected a 1–3 % decline in U.S. wind speeds by mid-century, while Davy et al. (2018) found no significant changes in the Black Sea region, and Chen et al. (2012) reported negligible changes in China by the end of the century. Tobin et al. (2016) projected modest increases (~5 %) in most European countries. These differences reflect regional circulation dynamics, large-scale teleconnections, and the influence of local topography and coastal processes, which are more pronounced along the Guinea coast than in mid-latitude continental settings.

Overall, the combination of observational validation, high-resolution modeling, and seasonal spatial analysis used here strengthens confidence in Togo's wind energy potential, particularly in northern, coastal, and highland zones. The alignment with regional projections supports strategic prioritization of these areas for wind farm development, while divergences from mid-latitude trends highlight the need for region-specific renewable energy planning.

5. Conclusion

The assessment of wind resources in Togo reveals The assessment of wind resources in Togo reveals a significant and spatially diverse potential that can strongly support the country's renewable energy ambitions. High-performing datasets such as MERRA-2 and regional climate models including MIROC, MPI, and ICHEC accurately capture historical wind dynamics, providing a solid foundation for robust future projections. The analysis shows that northern Togo concentrates the most favorable seasonal wind regimes, with considerable peaks during the rainy season, while central areas exhibit moderate but exploitable wind conditions and the southern coastal zone benefits from stable winds maintained by persistent sea breezes. Seasonal variability remains pronounced, with maximum wind speeds and power densities occurring between June and August and lower values during the dry season, underscoring the relevance of hybrid wind–solar systems to ensure year-round reliability. Looking ahead, projected increases in wind speed of 4–8% translate into notable improvements in wind power density, particularly in the northern and central regions, marking vast opportunities for energy expansion by 2040. These findings collectively point to strategic pathways for energy planning, including the development of large-scale northern wind farms, hybrid coastal installations, and the exploitation of local microclimates supported by storage and hybridization solutions. Overall, this study establishes a comprehensive and data-driven framework to guide the effective deployment of wind energy in Togo, enabling the country to capitalize on its regional and seasonal wind dynamics while advancing national renewable energy and sustainable development goals**.**

Références

Abdraman, M., Tahir, A., Lissouck, D., Kazet, M., & Mouangue, R. (2016). Wind resource assessment in the city of N'djamena in Chad. *International Journal of Renewable Energy Research, 6*, 1022–1036. https://doi.org/10.20508/ijrer.v6i3.4066.g6885

Abolude, A. T., Zhou, W., & Akinsanola, A. A. (2020). Evaluation and projections of wind power resources over China for the energy industry using CMIP5 models. *Energies, 13*, 2417. https://doi.org/10.3390/en13102417

Akinsanola AA, Ogunjobi KO, Abolude AT, Sarris SC, Ladipo KO (2017) Assessment of Wind Energy Potential for Small Communities in South-South Nigeria: Case Study of Koluama, Bayelsa State. J Fundam Renewable Energy Appl 7: 227. https://doi.org/10.4172/20904541.1000227

Allouhi, A., Zamzoum, O., Islam, M. R., et al. (2017). Evaluation of wind energy potential in Morocco's coastal regions. *Renewable and Sustainable Energy Reviews, 72*, 311–324. https://doi.org/10.1016/j.rser.2017.01.047

Arreyndip, N. A., Joseph, E., & David, A. (2016). Wind energy potential assessment of Cameroon's coastal regions for the installation of an onshore wind farm. *Heliyon, 2*, e00187. https://doi.org/10.1016/j.heliyon.2016.e00187

Asfaw, A., Simane, B., Hassen, A., & Bantider, A. (2018). Variability and Time Series Trend Analysis of Rainfall and Temperature in Northcentral Ethiopia: A Case Study in Woleka Sub-Basin. *Weather and Climate Extremes, 19*, 29–41. https://doi.org/10.1016/j.wace.2017.12.002

Ayodele, T. R., Jimoh, A. A., Munda, J. L., & Agee, J. T. (2012). Wind distribution and capacity factor estimation for wind turbines in the coastal region of South Africa. *Energy Conversion and Management, 64*, 614–625. https://doi.org/10.1016/j.enconman.2012.06.007

Batablinle, L., Lawin, E. and Agnide, S. (2018) Africa-Cordex Simulations Projection of Future Temperature, Precipitation, Frequency and Intensity Indices Over Mono Basin in West

Africa. Journal of Earth Science & Climatic Change, 9, 1-12. https://doi.org/10.4172/2157-7617.1000490

Batablinlè, L., Kongnine, D. M., Panafeïkow, P., Kossi, T., Yendoubé, L., Zakaria, D., Lawin, A. E., & Banna, M. (2025). Modeling and optimization of hybrid hydro-solar-wind systems for green hydrogen production in Togo. *International Journal of Renewable Energy Development, 14*(4), 813-828. https://doi.org/10.61435/ijred.2025.61136

Bandoc, G., Prăvălie, R., Cristian, P., & Mircea, D. (2018). Spatial assessment of wind power potential at global scale. A geographical approach. *Journal of Cleaner Production, 200*, 1065–1086. https://doi.org/10.1016/j.jclepro.2018.07.288

Breslow, P. B., & Sailor, D. J. (2002). Vulnerability of wind power resources to climate change in the continental United States. *Renewable Energy, 27*, 585–598. https://doi.org/10.1016/S0960-1481(01)00110-0

Boudia, S. M., Benmansour, A., & Hellal, M. A. T. (2016). Wind resource assessment in Algeria. *Sustainable Cities and Society, 22*, 171–183. https://doi.org/10.1016/j.scs.2016.02.010

Célestin, M., Emmanuel, L., Batablinlè, L., & Marc, N. (2019). Spatio-Temporal Analysis of Climate Change Impact on Future Wind Power Potential in Burundi (East Africa). *American Journal of Climate Change, 8*, 237–262. https://doi.org/10.4236/ajcc.2019.82014

Chen, Z., Li, W., Guo, J., Bao, Z., Pan, Z., & Hou, B. (2020). Projection of wind energy potential over northern China using a regional climate model. *Sustainability, 12*, 3979. https://doi.org/10.3390/su12103979

Davy, R., Gnatiuk, N., Pettersson, L., & Bobylev, L. (2018). Climate change impacts on wind energy potential in the European domain with a focus on the Black Sea. *Renewable and Sustainable Energy Reviews, 81*, 1652–1659. https://doi.org/10.1016/j.rser.2017.05.253

Elmabruk, A. M., Aleej, F. A., & Badii, M. M. (2014). Estimation of wind energy in Libya 2014: 5th International Renewable Energy Congress (IREC). IEEE, 1–6.

Lagili, H. S. A., Kiraz, A., Kassem, Y., & Gökçekuş, H. (2023). Wind and Solar Energy for Sustainable Energy Production for Family Farms in Coastal Agricultural Regions of Libya Using Measured and Multiple Satellite Datasets. *Energies*, *16*(18), 6725. https://doi.org/10.3390/en16186725

Elsner, P. (2019). Continental-scale assessment of the African offshore wind energy potential: Spatial analysis of an under-appreciated renewable energy resource. *Renewable and Sustainable Energy Reviews, 104*, 394–407. https://doi.org/10.1016/j.rser.2019.01.034

Eyring, V., Bony, S., Meehl, G. A., Senior, C. A., Stevens, B., Stouffer, R. J., and Taylor, K. E.: Overview of the Coupled Model Intercomparison Project Phase 6 (CMIP6) experimental design and organization, Geosci. Model Dev., 9, 1937–1958, https://doi.org/10.5194/gmd-9-1937-2016

Fant, C., Schlosser, C. A., & Strzepek, K. (2016). The impact of climate change on wind and solar resources in southern Africa. *Applied Energy, 161*, 556–564. https://doi.org/10.1016/j.apenergy.2015.03.042

George, Y. L., & David, W. W. (2008). An Adaptive Inverse-Distance Weighting Spatial Interpolation Technique. *Computers & Geosciences, 34*, 1044–1055. https://doi.org/10.1016/j.cageo.2007.07.010

Giorgi, Giorgi, F. (2009) Simulation of Regional Climate Using a Limited Area Model Nested in a General Circulation Model. Journal of Climate, 3, 941-963. https://doi.org/10.1175/1520-0442(1990)003<0941:SORCUA>2.0.CO;2

Guo, J., Huang, G., Wang, X., Xu, Y., & Li, Y. (2019). Projected changes in wind speed and its energy potential in China using a high-resolution regional climate model. *Wind Energy, 23*, 471–485. https://doi.org/10.1016/j.accre.2021.06.005

Hueging, H., Haas, R., Born, K., Jacob, D., & Pinto, J. G. (2013). Regional changes in wind energy potential over Europe using regional climate model ensemble projections. *Journal of Applied Meteorology and Climatology, 52*, 903–917. https://doi.org/10.1175/JAMC-D-12-086.1

IRENA. (2020). Renewable Energy Statistics 2020. International Renewable Energy Agency, Abu Dhabi.

Kulkarni, S., & Huang, H. P. (2014). Changes in surface wind speed over North America from CMIP5 model projections and implications for wind energy. *Advances in Meteorology, 2014*, 1–10. https://doi.org/10.1155/2014/292768

Lamboni, B., Bazyomo, S. D., Badouc, F. D., Hounkpe, J., Kamou, H., Zakari, D., Banna, M., & Lawin, A. E. (2024). Climate, water, hydropower, wind speed and wind energy potential resources assessments using weather time series data, downscaled regional circulation models: A case study for Mono River Basin in the Gulf of Guinea region. *Journal of Renewable Energy*. https://doi.org/10.1016/j.renene.2024.120099

Lamboni, B., Lawin, A. E. (2024). Time series analysis and forecasting of streamflow at Nangbeto dam in Mono Basin using stochastic approaches. *World Journal of Advanced Research and Reviews, 23*(2), 754–762. https://doi.org/10.30574/wjarr.2024.23.2.2375

Lamboni, B., M'po, Y. N., & Lawin, A. E. (2024). Vulnerability of water resources to drought risk and flood prevention in Mono River Basin (Gulf of Guinea Region). *International Journal of Advanced Research, 12*(07), 347–359. https://dx.doi.org/10.21474/IJAR01/19062

Landry, M., Ouedraogo, Y., Gagnon, Y., & Ouedraogo, A. (2017). On the wind resource mapping of Burkina Faso. *International Journal of Green Energy, 14*, 150–156. https://doi.org/10.1080/15435075.2016.1253571

Meishen Li, & Xianguo Li. (2005). Investigation of wind characteristics and assessment of wind energy potential for Waterloo region, Canada. *Energy Conversion and Management, 46*, 3014–3033. DOI:10.1016/j.enconman.2005.02.011

Mentis, D., Hermann, S., Howells, M., Welsch, M., & Siyal, S. H. (2015). Assessing the technical wind energy potential in Africa: a GIS-based approach. *Renewable Energy, 83*, 110–125. https://doi.org/10.1016/j.renene.2015.03.072

Monjid, A., Maach, A., Elghanami, D., & Hafid, A. (2015). Wind resource assessment: north and west of Morocco. 3rd International Renewable and Sustainable Energy Conference (IRSEC), IEEE, 1–6.

Mukasa, A. D., Mutambatsere, E., Arvanitis, Y., & Triki, T. (2013). Continental-scale assessment of the African offshore wind energy potential: Spatial analysis of an under-appreciated renewable energy resource. Working Paper 170-Development of Wind Energy in Africa, 449.

Olaofe, Z. O. (2018). Review of energy systems deployment and development of offshore wind energy resource map at the coastal regions of Africa. *Energy, 161*, 1096–1114. https://doi.org/10.1016/j.energy.2018.08.082

Safari, B., & Gasore, J. (2010). A statistical investigation of wind characteristics and wind energy potential based on the Weibull and Rayleigh models in Rwanda. *Renewable Energy, 35*, 2874–2880. https://doi.org/10.1016/j.renene.2010.05.006

Sawadogo, W., Abiodun, B. J., & Okogbue, E. C. (2019). Projected changes in wind energy potential over West Africa under the global warming of 1.5 °C and above. *Theoretical and Applied Climatology, 138*, 321–333. https://doi.org/10.1007/s00704-019-02853-5

Sawadogo, W., et al. (2020). Current and future potential of solar and wind energy over Africa using the RegCM4 CORDEX-CORE ensemble. *Climate Dynamics, 1–26*. https://doi.org/10.1007/s00382-020-05350-y

Soares, P. M., Lima, D. C., Semedo, A., Cabos, W., & Sein, D. V. (2019). Climate change impact on Northwestern African offshore wind energy resources. *Environmental Research Letters, 14*, 124065. https://doi.org/10.1088/1748-9326/ab573d

Stouffer, R. J., Eyring, V., Meehl, G. A., Bony, S., Senior, C., Stevens, B., & Taylor, K. E. (2017). CMIP5 scientific gaps and recommendations for CMIP6. *Bulletin of the American Meteorological Society, 98*, 95–105. https://doi.org/10.1175/BAMS-D-15-00008.1

Tobin, I., Vautard, R., Balog, I., Bréon, F.-M., Jerez, S., Ruti, P. M., Thais, F., Vrac, M., & Yiou, P. (2015). Assessing climate change impacts on European wind energy from ENSEMBLES high-resolution climate projections. *Climatic Change, 128*, 99–112. https://doi.org/10.1007/s10584-014-1291-0

Udo, N. A., Oluleye, A., & Ishola, K. A. (2017). Investigation of wind power potential over some selected coastal cities in Nigeria.

Innovative Energy Research, 6, 156. https://doi.org/10.4172/2090-5004.1000156

Wang, X., Huang, G., & Liu, J. (2016). Twenty-first century probabilistic projections of precipitation over Ontario, Canada through a regional climate model ensemble. *Climate Dynamics, 46*, 3979–4001. https://doi.org/10.1007/s00382-015-2825-5

Zheng, C. W., Li, X. Y., Luo, X., Chen, X., Qian, Y. H., Zhang, Z.-H., Gao, Z.-S., Du, Z.-B., Gao, Y.-B., & Chen, Y.-G. (2019). Projection of future global offshore wind energy resources using CMIP data. *Atmosphere-Ocean, 57*, 134–148. https://doi.org/10.1080/07055900.2018.1543984